

Articles

Fluorescence Properties and Photoisomerization Behavior of 1-(9-Anthryl)-2-(2-quinolinyl)ethene

Eun Ju Shin

Department of Chemistry, Sunchon National University, Sunchon, Chonnam 540-742, Korea

Received August 5, 1999

The fluorescence properties and photoisomerization behavior of 1-(9-anthryl)-2-(2-quinolinyl)ethene (2-AQE) have been investigated in various solvents. Instead of phenyl ring in 1-(9-anthryl)-2-phenylethene, the introduction of quinoline ring reduces not only the fluorescence yield but also the photoisomerization yield, due to competition of efficient radiationless deactivation and an increase in the torsional barrier for twisting in the singlet manifold. The S_1 decay parameters were found to be solvent-dependent due to the charge-transfer character of lowest S_1 state. Polar solvents reduce the activation barrier to twisting, thus slight enhancing the isomerization of t-2-AQE in the singlet manifold. As solvent polarity is increased, Φ_f of c-2-AQE is greatly reduced, but $\Phi_{c \rightarrow t}$ is practically independent of solvent polarity. Dual fluorescence in t-2-AQE was observed and two fluorescing species could be assigned t-2-AQE and c-2-AQE, where the ratio between two species was dependent on the solvent polarity. Interestingly, in the concentration above 1×10^{-4} M, the shapes of the fluorescence excitation spectra of t- and c-2-AQE are significantly altered without spectral changes of their fluorescence and absorption, probably due to the formation of excimer.

Introduction

The excited-state properties of 1-(n-anthryl)-2-phenylethenes (n-APEs, with $n = 1, 2,$ and 9) have been widely studied because they accomplish efficient *cis* \rightarrow *trans* photoisomerization, but do not undergo reverse *trans* \rightarrow *cis* photoisomerization.¹⁻⁶ *Cis* \rightarrow *trans* photoisomerization of c-9-APE occurs via triplet adiabatic pathway ($^3c^* \rightarrow ^3t^* \rightarrow t$) in non-polar solvent and singlet diabatic/adiabatic mixed pathway ($^1c^* \rightarrow ^1p^* \rightarrow p \rightarrow t$ or $^1c^* \rightarrow ^1t^* \rightarrow t$) in polar solvent.⁷ The energy barrier to twisting is too high for t-9-APE to undergo *trans* \rightarrow *cis* photoisomerization. The excitation energy is extensively localized in the large anthracene moiety so that the transoid geometry corresponds to energy minima in the excited potential energy surface. Interestingly, 9-APE derivatives bearing polar substituents in the para position of the styryl group are known to undergo *trans* \rightarrow *cis* photoisomerization due to the lowering of the torsional barrier for twisting in the singlet manifold *via* the intramolecular charge transfer processes, especially in polar solvent.⁸⁻¹³

However, although the effect of the nitrogen heteroatom on the excited state properties of stilbene-like molecules has been extensively studied,¹⁴⁻¹⁸ much less is known about the excited state behavior of n-APE derivatives containing the nitrogen heteroatom.¹⁹ For compounds bearing pyridine rings, the proximity effect of the lowest π, π^* state and a close-lying n, π^* state in the singlet manifold can lead to efficient $S_1 \rightarrow S_0$ internal conversion (IC), thus affecting the relaxation properties and photoisomerization behavior of aza-stilbenes.

In comparison with parent 9-APE, the aza substitution changes the donor-acceptor properties of the molecules.¹⁹⁻²¹

Therefore, aza-derivatives of 9-APE are expected to undergo *trans* \rightarrow *cis* photoisomerization by way of intramolecular charge-transfer processes. The excited state properties of some pyridyl²⁰ and pyrazinyl derivatives²¹ of 9-APE have been previously investigated. As reported in our previous papers, 1-(9-anthryl)-2-(n-pyridyl)ethenes (n-APyE, $n = 2$ or 4), mono-aza analogues of 9-APE, show efficient *trans* \rightarrow *cis* photoisomerization in polar solvent, and 1-(9-anthryl)-2-pyrazinyl-ethene (APzE), a di-aza analogue of 9-APE, exhibits *trans* \rightarrow *cis* photoisomerization even in nonpolar solvent.

From the viewpoint of correlating the photophysical properties and photoisomerization behavior of 1-(9-anthryl)-2-arylethenes with the size and aza substitution of aryl groups, our study is extended to a quinolinyl derivative containing two polycyclic aryl groups. The present work deals with the properties of the excited state of t-2-AQE and c-2-AQE using steady state emission spectroscopy and photochemical behavior. The results are discussed in comparison with the previous results of phenyl,³⁻⁷ naphthyl,^{4,5} pyridyl,²⁰ and pyrazinyl²¹ derivatives of 1-(9-anthryl)-2-arylethenes.

Experimental Section

Reagents. For spectroscopic measurements and photochemical reactions, n-hexane, tetrahydrofuran (THF), ethyl acetate (EtOAc), acetonitrile (CH₃CN), and methanol (MeOH) of HPLC grade (Merck) were used. Methylcyclohexane (MCH) and ethanol (EtOH) (Aldrich) are used of spectrophotometric grade. Dichloromethane (CH₂Cl₂) and toluene are freshly distilled from P₂O₅ and CaH₂, respectively. All other chemicals are used as received.

Synthesis. The synthesis of 2-AQE was accomplished by Wittig reaction between 9-anthrylmethyltriphenylphosphonium bromide and 2-quinolinecarboxaldehyde. In dimethyl sulfoxide (50 mL) solution of 9-anthrylmethyltriphenylphosphonium bromide (1.33 g, 2.5 mmol) and 2-quinolinecarboxaldehyde (0.31 g, 2 mmol), sodium methoxide (0.14 g, 2.5 mmol) was added and stirred at 80 °C for 5 hrs. The resulting mixture was poured into distilled water and extracted three times with ethyl ether. The combined ether layer was rinsed several times with distilled water and dried with anhydrous magnesium sulfate. The solution was concentrated in vacuo and separated with silica gel column chromatography using hexane/ethyl acetate = 10/1 (v/v) as an eluent. The first fraction contained triphenylphosphine oxide (Ph₃PO). T-2-AQE (136.4 mg, 0.4 mmol, 20% yield) and c-2-AQE (160 mg, 0.5 mmol, 25% yield) were obtained in the second and third fraction, respectively.

t-2-AQE (bright yellow solid); mp.: 170-172 °C. IR: 1592, 1505, 1424, 1116, 988, 885, 846, 818, 778, 737 cm⁻¹. ¹H NMR (CDCl₃): δ 7.27 (1H, d, *J* = 16.3 Hz, H10), 7.45-7.48 (4H, m, H2', 3', 6', 7'), 7.51-7.54 (1H, d, H6), 7.72-7.75 (2H, m, H3, 5), 7.79-7.82 (1H, m, H7), 7.98-8.02 (2H, m, H4', 5'), 8.14-8.18 (2H, m, H4, 8), 8.39-8.43 (3H, m, H1', 8', 10'), 8.60 (1H, d, *J* = 16.3 Hz, H9).

c-2-AQE (orange solid); mp.: 111-113 °C. IR: 1617, 1594, 1501, 1307, 1114, 1014, 892, 836, 810, 788, 770, 734 cm⁻¹. ¹H NMR (CDCl₃): δ 6.41 (1H, d, *J* = 8.9 Hz, H10), 7.28 (1H, d, *J* = 8.9 Hz, H9), 7.32-7.40 (4H, m, H2', 3', 6', 7'), 7.41-7.46 (2H, m, H3, 6), 7.57-7.64 (3H, m, H4, 5, 7), 8.00 (2H, d, *J* = 7.8 Hz, H4', 5'), 8.03 (1H, d, *J* = 7.8 Hz, H8), 8.22 (2H, d, *J* = 8.7 Hz, H1', 8'), 8.45 (1H, s, H10').

Spectroscopic and photochemical measurements. ¹H NMR spectra were measured on 300 MHz Varian UNITY plus 300 spectrometer in chloroform-*d*₁. IR spectra were obtained in KBr pellets on Midac Prospect-IR spectrometer. Absorption spectra were recorded on a Hitachi U-3210 spectrophotometer. Steady state emission spectra were recorded on a SLM-AMINCO AB2 luminescence spectrometer. SPEX Fluorolog-T2 was used for the measurement of fluorescence lifetimes. HPLC was accomplished using Waters Nova-Pak C18 analytical column on a HPLC system equipped with Waters 510 pump and Young-In M720 absorbance detector. Experimental details for measurements of quantum yields of fluorescence and photoisomerization were described previously.^{20,21}

Results and Discussion

Absorption spectra. The absorption spectra of *t*-2-AQE and *c*-2-AQE in *n*-hexane and methanol are represented in Figure 1. The absorption spectrum of trans isomer is broad, while cis isomer shows more structured and weaker absorption. The absorption maxima in acetonitrile are 391 nm ($\epsilon = 14,960$) for *t*-2-AQE and 391 ($\epsilon = 9,000$), 370 ($\epsilon = 9,010$), and 353 ($\epsilon = 6,560$) nm for *c*-2-AQE. The absorption maxima of *t*-2-AQE and *c*-2-AQE in the solvents of various polarity, which appear to be insensitive to the medium, are represented in Tables 1 and 2, respectively, along with some

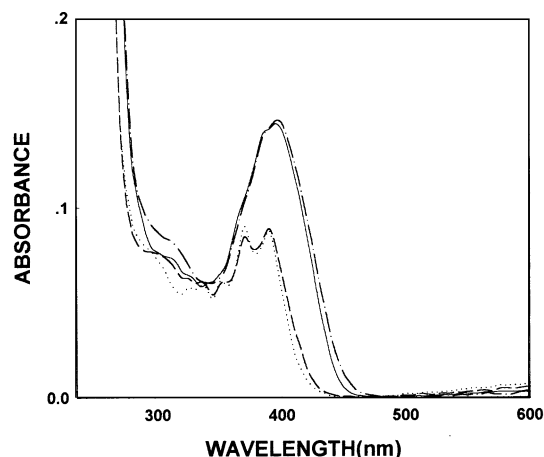


Figure 1. Absorption spectra of *t*- and *c*-2-AQE in hexane (solid line for *t*-2-AQE, dotted line for *c*-2-AQE) and methanol (dash-dotted line for *t*-2-AQE, dashed line for *c*-2-AQE) at room temperature.

photophysical and photochemical properties.

Tables 3 and 4 show the photophysical and photochemical properties of *t*-2-AQE and *c*-2-AQE in comparison with those of 1-(9-anthryl)-2-phenylethene(9-APE)^{3,6-9,13} and its aza derivatives 1-(9-anthryl)-2-(*n*-pyridyl)ethene(*n* = 2, 3, or 4, *n*-APyEs)²⁰ and 1-(9-anthryl)-2-pyrazinylethene(APzE),²¹ and 1-(9-anthryl)-2-(1-naphthyl)ethene(1-ANE)⁵ in *n*-hexane and acetonitrile. Absorption spectra of 2-AQE are similar to those of 9-APE and 1-ANE except that the maxima are slightly red-shifted. The first intense absorption band of *t*-2-AQE is placed at approximately 394 nm corresponding to the band at 388 nm of *t*-9-APE and *t*-1-ANE in *n*-hexane. The introduction of the quinoline ring results in a bathochromic shift with respect to the conjugation band of 9-APE and 1-ANE.

Fluorescence spectra. Figure 2 shows normalized fluorescence spectra of *t*-2-AQE and *c*-2-AQE in *n*-hexane and methanol. Fluorescence spectra of *t*-2-AQE and *c*-2-AQE in *n*-hexane at room temperature show very similar and structureless shapes but fluorescence maximum of *t*-2-AQE (483 nm) is slightly longer than that of *c*-2-AQE (480 nm). Fluorescence properties of *t*-2-AQE and *c*-2-AQE are strongly solvent-dependent. Fluorescence of *t*-2-AQE in methanol is pronouncedly red-shifted with respect to that in *n*-hexane. Fluorescence of *c*-2-AQE in methanol is too weak to mea-

Table 1. Absorption maxima (λ_a^{\max}), fluorescence maxima (λ_f^{\max}), quantum yields (Φ_f), lifetimes (τ_f), and photoisomerization quantum yields ($\Phi_{t \rightarrow c}$) of *t*-2-AQE in various solvents at room temperature

solvent	λ_a^{\max} , nm (ϵ_{\max})	λ_f^{\max} , nm	τ_{f1} (%), ns	τ_{f2} (%), ns	Φ_f	$\Phi_{t \rightarrow c}$
hexane	394(14,500)	483	2.53(90)	0.46(10)	0.41	<0.01
toluene	397(10,200)	499	2.02(75)	0.47(25)	0.29	-
THF	399(14,300)	498	1.03(62)	0.43(38)	0.18	0.09
EtOAc	395(13,300)	497	1.28(61)	0.37(39)	0.13	0.12
CH ₂ Cl ₂	400(13,200)	502	1.03(20)	0.37(80)	0.08	0.15
CH ₃ CN	391(15,000)	502	0.84(7)	0.19(93)	0.04	0.15
EtOH	397(15,400)	505	1.88(3)	0.14(97)	0.03	0.10
MeOH	394(14,700)	518	2.35(3)	0.09(97)	0.02	0.09

Table 2. Absorption maxima (λ_a^{\max}), fluorescence maxima (λ_f^{\max}), quantum yields (Φ_f), lifetimes (τ_f), and photoisomerization quantum yields ($\Phi_{c \rightarrow t}$) of c-2-AQE in various solvents at room temperature

solvent	λ_a^{\max} , nm (ϵ^{\max})	λ_f^{\max} , nm	τ_f , ns ^a	Φ_f	$\Phi_{c \rightarrow t}$
hexane	389(8,800)	480	0.46	0.39	-
	369(8,600)				
	350(5,900)				
toluene	392(9,100)	497	0.47	0.23	0.22
	372(8,600)				
	355(5,800)				
THF	391(8,900)	498	0.43	0.044	0.22
	371(8,600)				
	338(5,800)				
EtOAc	389(9,200)	498	0.37	0.041	0.22
	371(9,000)				
	350(6,500)				
CH ₂ Cl ₂	391(9,500)	506	0.37	0.012	0.24
	372(9,100)				
	354(6,500)				
CH ₃ CN	391(9,000)	498	0.19	0.006	0.18
	370(9,000)				
	353(6,600)				
EtOH	390(9,300)	506	0.14	0.008	0.16
	370(8,800)				
	352(6,400)				
MeOH	388(8,300)	507	0.09	0.004	0.17
	369(7,500)				
	338(5,200)				

^aTaken from τ_{f2} values in Table 1.

sure. As shown in Table 1, fluorescence maximum of t-2-AQE is red-shifted and fluorescence quantum yield is markedly decreased with increasing the solvent polarity. Fluorescence of c-2-AQE (Table 2) is more rapidly weakened than that of t-2-AQE with the solvent polarity and has not been easily detected in solvents more polar than tetrahydrofuran. Lower fluorescence quantum yield of c-2-AQE than that of t-2-AQE indicates the barrierless twisting around ethenic bond in cis isomer.

In Tables 3 and 4, some photophysical and photochemical parameters of *trans* and *cis* isomers of 1-(9-anthryl)-2-arylethenes are collected and compared with those of 2-AQE. Parameters for n-APyEs and APzE are published data from our laboratory.^{20,21} Data for 9-APE^{3,6-9,13} and 1-ANE^{4,5} are taken from literature. As shown in Tables 3 and 4, fluorescence maxima of t-2-AQE and c-2-AQE are slightly longer than those of other 9-APE derivatives. Fluorescence quantum yield of t-2-AQE in n-hexane is somewhat lower than or similar to those of t-9-APE, t-n-APyE, and t-1-ANE, even if a little higher than that of t-APzE. In acetonitrile, fluorescence quantum yield of t-2-AQE is much lower than of t-9-APE and t-3-APyE, but similar to those of t-n-APyE (n = 2, 4) and t-APzE. As in the case of other aza derivatives of 9-APE, for 2-AQE the intramolecular charge transfer is likely to be responsible for the decrease of the fluorescence yield in polar solvents. As the solvent polarity is increased, the twisted state on the excited energy surface, which has

Table 3. Photophysical and photochemical parameters of some t-1-(9-anthryl)-2-arylethenes at room temperature

compound	solvent	λ_a^{\max} , nm (ϵ^{\max})	λ_f^{\max} , nm	Φ_f	τ_f , ns	$\Phi_{t \rightarrow c}$
t-9-APE	MCH	385(11,220) 405(6,900) ^a	468 ^b	0.44 ^c	3.6 ^c	<0.01 ^d
	CH ₃ CN	385(11,200)	476 ^b	0.45 ^c	4.3 ^c	0.003 ^d
t-2-APyE ^e	hexane	387(16,600) 410(10,100)	473	0.49	3.5	<0.01
	CH ₃ CN	389(15,500)	487	0.08	0.9	0.44
t-3-APyE ^e	hexane	387(10,200)	475	0.43	3.7	<0.01
	CH ₃ CN	400(8,600) 391(10,600)	480	0.38	3.6	<0.01
t-4-APyE ^e	hexane	386(11,200)	476	0.44	3.6	<0.01
	CH ₃ CN	386(12,000)	493	0.04	0.3	0.37
t-APzE ^f	hexane	395(12,600) 384(11,900) 363(8,700)	472	0.37	3.3	0.07
	CH ₃ CN	400(12,700) 391(13,100) 371(10,300)	494	0.03	-	0.20
	toluene	388	504	0.44	5.54	<0.001
	hexane	394(14,500)	483	0.41	2.53, 0.49	<0.01
t-2-AQE	CH ₃ CN	391(15,000)	502	0.04	0.84, 0.19	0.15

^aTaken from ref. 3. ^bTaken from ref. 9. ^cTaken from ref. 6. ^dTaken from ref. 8. ^eTaken from ref. 20. ^fTaken from ref. 21. ^gTaken from ref. 5.**Table 4.** Photophysical and photochemical parameters of some c-1-(9-anthryl)-2-arylethenes at room temperature

compound	solvent	λ_a^{\max} , nm (ϵ^{\max})	λ_f^{\max} , nm	Φ_f	τ_f (%), ns	$\Phi_{c \rightarrow t}$
c-9-APE ^a	MCH	388 ^b	460	0.16	2.2(88), 3.6(12)	0.19
	CH ₃ CN	388 ^b	469	0.05	0.13(35), 4.2(65)	0.41
c-2-APyE ^c	hexane	388(6,200) 368(6,600) 351(4,000) 334(1,800)	468	0.14	-	0.13 ^e
	CH ₃ CN	389, 370, 352, 334	487	0.02	-	0.19
c-4-APyE ^c	hexane	388, 368(6,000), 353, 342	463	0.20	-	0.27 ^e
	CH ₃ CN	390(4,900), 368, 350	490	0.004	-	0.21
c-APzE ^d	hexane	390(7,400) 370(7,500) 352(5,200) 335(3,400)	470	0.24	-	0.31
	CH ₃ CN	389(6,270) 370(13,100) 351(4,400)	482	0.002	-	0.25
c-2-AQE	hexane	389(8,800)	480	0.39	0.46	0.22 ^e
	CH ₃ CN	391(9,000)	498	0.006	0.19	0.18

^aTaken from ref. 7. ^bTaken from ref. 8. ^cTaken from ref. 20. ^dTaken from ref. 21. ^eData in toluene.

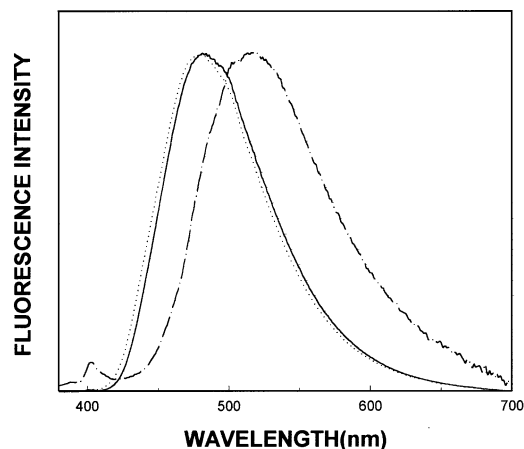


Figure 2. Normalized fluorescence spectra of t- and c-2-AQE in hexane (solid line for t-2-AQE, dotted line for c-2-AQE) and methanol (dash-dotted line for t-2-AQE) at room temperature.

zwitterionic character, is more stabilized through the intramolecular charge transfer and the photoisomerization from either trans or cis side becomes more feasible, and thus fluorescence efficiency is decreased.

As shown in Tables 3 and 5, for t-9-APE fluorescence becomes intense, blue-shifted, and more structured on going from room temperature ($\lambda_f = 468$ nm, $\Phi_f = 0.44$ in methylcyclohexane-3-methylpentane 9/1 (v/v) (MCH-3MP))^{6,9} to 77 K ($\lambda_f = 438, 460$ nm, $\Phi_f = 0.48$ in 2,2-dimethylbutane-n-pentane 8/3 (v/v) (D-P)).⁹ Fluorescence of c-9-APE in MCH-3MP becomes intense, blue-shifted, but still broad with decreasing temperature from room temperature ($\lambda_f = 460$ nm, $\Phi_f = 0.16$)⁷ to 77 K ($\lambda_f = 425$ nm, $\Phi_f = 0.57$).^{6,7} However, contrary to 9-APE, the fluorescence spectra of t-2-AQE ($\lambda_f = 475$ nm, $\Phi_f = 0.32$ in MCH) and c-2-AQE ($\lambda_f = 475$ nm, $\Phi_f = 0.34$ in MCH) in a rigid matrix at 77 K (Figure 3 and Table 5), which are almost independent of solvent polarity, have very similar and broad structureless shapes, although blue-shifted with respect to those at room temperature ($\lambda_f = 483$ nm for t-2-AQE, 480 nm for c-2-AQE in n-hexane) (Tables 1, 2). The geometrical structures of t-2-AQE as well as c-2-AQE should quite deviate from the planarity even at 77 K. The fluorescence quantum yield at 77 K remains substantially below unity (0.29-0.39), thus indicating an efficient intersystem crossing.

The absorption and fluorescence spectral shapes of t- and

Table 5. Fluorescence maxima (λ_f^{\max}) and quantum yields (Φ_f) of t- and c-2-AQE at 77 K in comparison with those of t- and c-9-APE

compound	MCH-3MP		EtOH	
	λ_f^{\max} , nm	Φ_f	λ_f^{\max} , nm	Φ_f
t-9-APE ^a	438, 460 ^c	0.48 ^c	434, 460	0.56
c-9-APE ^b	468 ^d	0.14 ^d	468	0.14
t-2-AQE	475	0.32	475	0.39
c-2-AQE	475	0.34	475	0.29

^aTaken from ref. 9. ^bTaken from ref. 6, 7, and 9. ^cData in 2,2-dimethylbutane-n-pentane 8/3 (v/v) (D-P). ^dData in methylcyclohexane-3-methylpentane 9/1 (v/v) (MCH-3MP).

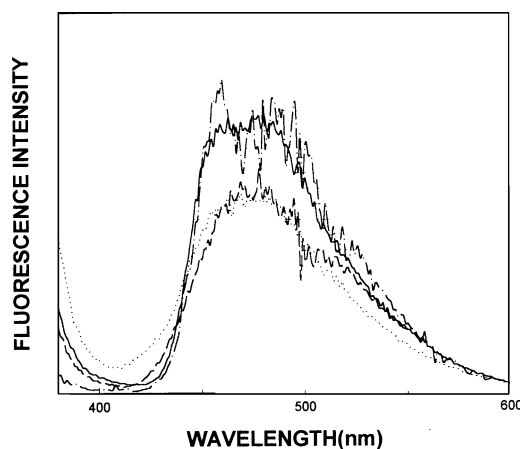


Figure 3. Fluorescence spectra of t- and c-2-AQE in methylcyclohexane (MCH) (solid line for t-2-AQE, dotted line for c-2-AQE) and ethanol (dash-dotted line for t-2-AQE, dashed line for c-2-AQE) at 77 K.

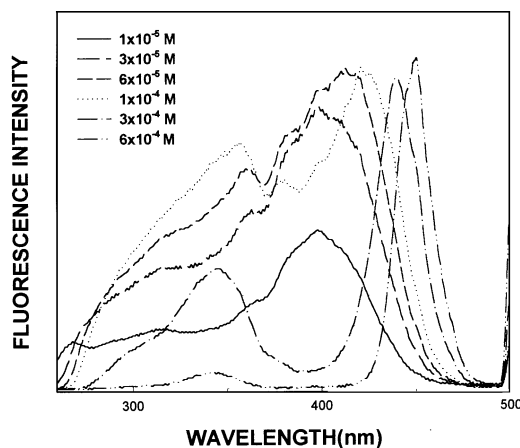


Figure 4. Concentration effect on excitation spectra of t-2-AQE in acetonitrile with $\lambda_f = 500$ nm.

c-2-AQE do not depend on the concentration. However, fluorescence is greatly quenched above the concentration of 1×10^{-4} M. Fluorescence excitation spectra of t- and c-2-AQE do not depend on the monitoring wavelength and the solvent polarity, but changes with the concentration. Figures 4 and 5 show the concentration effect on the excitation spectra of t-2-AQE and c-2-AQE in acetonitrile, respectively. In dilute solution around 1×10^{-5} M, the excitation spectra of t- and c-2-AQE are similar to their absorption spectra. But, at higher concentration than 1×10^{-4} M, fluorescence excitation spectral shapes of both t- and c-2-AQE are significantly altered and the longest absorption band maxima are gradually shifted to the longer wavelength as the concentration is increased. This is probably due to the intermolecular excimer formation. However, any excimer fluorescence is not observed. The concentration-dependent changes for the fluorescence excitation spectrum have not been yet observed in other 9-APE derivatives such as 9-APE, n-APyE, and APzE.

Fluorescence lifetimes. It was reported that the bi-exponential fluorescence decay of c-9-APE was observed above 300 K in non-polar solvent, 9/1 (v/v) MCH-3MP.⁷ The shorter

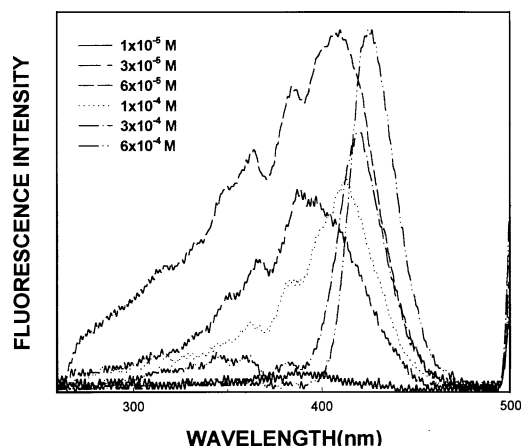
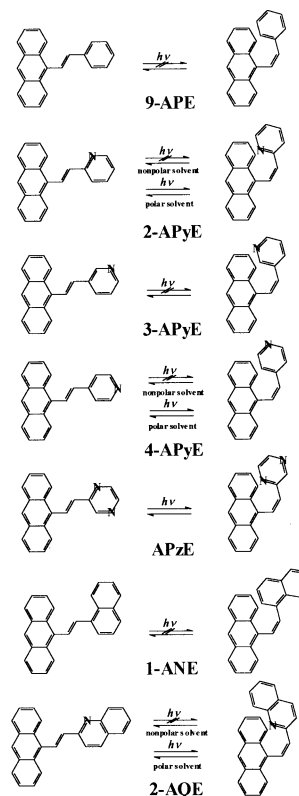


Figure 5. Concentration effect on excitation spectra of *c*-2-AQE in acetonitrile with $\lambda_f = 500$ nm.

lifetime (2.2 ns, 88%, major component at 293 K) was assigned to the 1c -9-APE* emission, while the longer lifetime (3.6 ns, 12%, at 293 K) was assigned to the 1t -9-APE* emission. In polar solvent (acetonitrile), the shorter lifetime (0.13 ns, 35%, at 293 K) decreased markedly and became minor component while the longer lifetime (4.2 ns, 65%, at 293 K) was more populated. This could be explained by a much faster 1c -9-APE* \rightarrow 1p * process in polar solvent due to a marked decrease of the torsional energy barrier.⁷ In contrast to the dual emission of *c*-9-APE, only monoexponential decay was observed in the fluorescence of *t*-9-APE.⁹

The fluorescence lifetimes of *t*-2-AQE in various solvents at room temperature are represented in Table 5. Fluorescence lifetime measurements using the phase modulation technique at room temperature show dual emission for *t*-2-AQE. In non-polar solvent, the long-lived component is major one. As the solvent polarity increases, the population of the long-lived component is decreased while the short-lived component is more populated. Both longer and shorter lifetimes are shortened in polar solvent. This could be explained by the efficient photoisomerization attributable to lowering of twisting barrier due to the stabilization of the intramolecular charge transfer state in polar solvents. These two species are tentatively assigned to 1t -2-AQE* (long-lived) and 1c -2-AQE* (short-lived). In the case of 9-APE, bi-exponential fluorescence decay has been suggested as a evidence of singlet adiabatic isomerization.⁷ Either the formation of the 1c -2-AQE* through the adiabatic pathway from 1t -2-AQE* or direct excitation of *c*-2-AQE formed by *trans* \rightarrow *cis* photoisomerization could contribute to short-lived component in the dual fluorescence of *t*-2-AQE.

Photoisomerization of *t*-2-AQE. The quantum yields of *trans* \rightarrow *cis* photoisomerization ($\Phi_{t \rightarrow c}$) of *t*-2-AQE upon 366 nm irradiation in solvents of a wide range of polarity are represented in Table 1. $\Phi_{t \rightarrow c}$ of *t*-2-AQE is slightly increased with the solvent polarity and then decreased in polar protic solvent. In Table 3, $\Phi_{t \rightarrow c}$ of *t*-2-AQE is compared with those of 9-APE,^{6,8} its aza derivatives *n*-APyEs,²⁰ APzE,²¹ and its polyaromatic derivative 1-ANE⁵ in hexane and acetonitrile. In nonpolar solvent, parent *t*-9-APE and *t*-*n*-APyE (*n* = 2-4)



Scheme 1. Photoisomerization of APE, APyEs, APzE, 1-ANE, and 2-AQE.

exhibit practically no photoisomerization, even if *t*-APzE undergoes inefficient but measurable photoisomerization. Similarly, *t*-2-AQE undergoes no *trans* \rightarrow *cis* photoisomerization in *n*-hexane and only a side photoreaction, which is considered to be photocyclization product, is observed. But, in more polar solvents, any side photoreaction cannot be observed and only the efficient photoisomerization occurs. As the solvent polarity increases, $\Phi_{t \rightarrow c}$ for *t*-9-APE remains still virtually zero.^{6,8} As the solvent polarity is increased, in our previous studies for *t*-*n*-APyE (*n* = 2, 4)²⁰ and *t*-APzE,²¹ the fluorescence quantum yield is decreased and photoisomerization quantum yield is complementarily increased due to the lowering of energy barrier against twisting in the excited state through the intramolecular charge-transfer. But, photoisomerization quantum yield of *t*-2-AQE is not noticeably increased, while the fluorescence quantum yield is significantly decreased with the solvent polarity. This can be explained that nonradiative decay processes become efficient in polar solvent due to the presence of the polycyclic aza-aromatic ring. $\Phi_{t \rightarrow c}$ and Φ_f of *t*-2-AQE show, even if partly, inverse relationship in varying the solvent polarity (Table 1). The excited state involved in *trans* \rightarrow *cis* photoisomerization of *t*-2-AQE is presumed to be a singlet excited state with the polar intramolecular charge transfer character as in some *t*-9-APE derivatives containing electron-donating and electron-withdrawing substituents,⁸⁻¹³ *t*-*n*-APyE (*n* = 2 or 4),²⁰ and *t*-APzE.²¹ However, the contribution of the triplet state to photoisomerization cannot be completely excluded. *T*-2-AQE exhibits less efficient photoisomerization in polar

protic solvent such as methanol. The hydrogen-bonding or protonation on the nitrogen atom in protic solvent could result in the decrease of the photoisomerization efficiency.

Polycyclic aza-aromatics are generally known to exhibit fast radiationless decay attributed by efficient internal conversion and intersystem crossing. The fact that $\Phi_{t \rightarrow c}$ of t-2-AQE is lower than those of t-n-APyE ($n = 2$ or 4) (Table 3) is probably due to more efficient nonreactive radiationless deactivation in t-2-AQE than in t-n-APyE ($n = 2$ or 4).

For t-n-APyE,²⁰ introduction of a nitrogen atom into phenyl moiety of 9-APE contributes to induce some change on the excited singlet energy surface. In other words, the activation barrier against twisting and/or the energy of the excited perpendicular state is lowered through intramolecular charge transfer process. This lowering leads to the enhancement of $\Phi_{t \rightarrow c}$ with Φ_f decreasing and τ_f being shortened. However, for t-2-AQE, substitution of quinoline ring instead of phenyl moiety in 9-APE induces not only lowering the activation barrier against on the excited singlet energy surface but also more efficient radiationless deactivation. In spite of Φ_f decreasing and τ_f being shortened, $\Phi_{t \rightarrow c}$ of t-2-AQE in polar solvent is only moderately increased and smaller than that of t-n-APyE ($n = 2$ or 4). It is probably due to competing the photoisomerization with efficient radiationless deactivation in the singlet manifold.

Photoisomerization of c-2-AQE. The quantum yield of *cis* \rightarrow *trans* photoisomerization ($\Phi_{c \rightarrow t}$) of c-2-AQE upon 366 nm irradiation at room temperature is represented in Table 2. In contrast to great decrease of Φ_f in polar solvents, $\Phi_{c \rightarrow t}$ of c-2-AQE is practically independent of solvent polarity in all solvents used except n-hexane, similar to $\Phi_{c \rightarrow t}$ of c-n-APyE ($n = 2$ or 4)²⁰ and c-APzE.²¹ This indicates that fluorescence and photoisomerization do not occur *via* common species. Triplet mechanism, at least partly, is suggested for *c* \rightarrow *t* photoisomerization. It is difficult to determine $\Phi_{c \rightarrow t}$ of c-2-AQE in n-hexane because of the complication by the formation of a side photoproduct with *trans* isomer, as in c-9-APE,⁷ c-n-APyE ($n = 2, 4$),²⁰ and c-APzE.²¹ It has been reported that c-9-APE undergoes efficient photoisomerization in polar solvents, but photocyclization is predominant process in nonpolar solvents.⁷ Moreover, the absorption ($\lambda_a = 357, 376, 395$ nm) and fluorescence ($\lambda_f = 404, 428, 450, 487$ nm) spectra of the side product from c-2-AQE are very similar to those ($\lambda_a = 347, 364, 384$ nm, $\lambda_f = 393, 416, 440, 471$ nm)⁷ of photocyclization product from c-9-APE. Therefore, we tentatively assigned this side product as a photocyclization product, although we cannot isolate and characterize this product because of low conversion and instability.

For c-9-APE, in nonpolar solvent (MCH-3MP) $\Phi_{c \rightarrow t}$ is relatively low (0.19) and the quantum yield of photocyclization (Φ_{cycl}) is relatively high (0.27) at room temperature, while in polar solvent (acetonitrile) $\Phi_{c \rightarrow t}$ is relatively high (0.41) and Φ_{cycl} is very low (0.045).⁷

Similar trend with the solvent polarity is observed for c-2-AQE. In all other solvents used except n-hexane, photoreaction of c-2-AQE seems to proceed cleanly to give only t-2-AQE. In polar solvents, photocyclization is completely inhibited

because more efficient photoisomerization effectively suppresses the photocyclization. It is proposed in n-hexane that photocyclization proceeds *via* the singlet manifold while photoisomerization occurs mainly by a triplet mechanism with contribution of some degree of singlet mechanism, due to substantial barrier to twisting in singlet manifold. As the solvent polarity is increased, torsional energy barrier on the singlet energy surface is decreased by the contribution of intramolecular charge transfer. Therefore, even in toluene photoisomerization occurs mostly in the singlet manifold while photocyclization product is not produced at all. Similar solvent-dependence on photoisomerization mechanism has been suggested for c-9-APE.⁷ In nonpolar solvents, photoisomerization of c-2-AQE occurs mainly by a triplet mechanism with contribution of some degree of singlet mechanism. In polar solvents, photoisomerization of c-2-AQE occurs mostly in the singlet manifold due to the decrease of torsional energy barrier on the singlet energy surface by the contribution of intramolecular charge transfer.

Acknowledgment. The author thanks Mr. Y. H. Lee for his technical assistance and Korea Basic Science Institute for the measurements of ¹H NMR and fluorescence lifetimes.

References

1. Arai, T.; Tokumaru, K. *Chem. Rev.* **1993**, *93*, 23.
2. Arai, T.; Tokumaru, K. *Adv. Photochem.* **1995**, *20*, 1.
3. Bartocci, G.; Masetti, F.; Mazzucato, U.; Spalletti, A.; Orlandi, G.; Poggi, G. *J. Chem. Soc. Faraday Trans. 2* **1988**, *84*, 385.
4. Bartocci, G.; Mazzucato, U.; Spalletti, A.; Orlandi, G.; Poggi, G. *J. Chem. Soc. Faraday Trans.* **1992**, *88*, 3139.
5. Bhattacharyya, K.; Chattopadhyay, S. K.; Baral-Tosh, S.; Das, P. K. *J. Phys. Chem.* **1986**, *90*, 2646.
6. Mazzucato, U.; Spalletti, A.; Bartocci, G. *Coord. Chem. Rev.* **1993**, *125*, 251.
7. Bartocci, G.; Spalletti, A.; Mazzucato, U. *Res. Chem. Intermed.* **1995**, *21*, 735.
8. Sandros, K.; Becker, H.-D. *J. Photochem.* **1987**, *39*, 301.
9. Gorner, H. *J. Photochem. Photobiol. A: Chem.* **1987**, *43*, 263.
10. Gorner, H.; Elisei, F.; Aloisi, G. *J. Chem. Soc. Faraday Trans.* **1992**, *88*, 29.
11. Sun, L.; Gorner, H. *J. Phys. Chem.* **1993**, *97*, 11186.
12. Sun, L.; Gorner, H. *Chem. Phys. Lett.* **1993**, *208*, 43.
13. Aloisi, G. G.; Elisei, F.; Latterini, L.; Passerini, M.; Galianzo, G. *J. Chem. Soc. Faraday Trans.* **1996**, *92*, 3315.
14. Mazzucato, U. *Pure Appl. Chem.* **1982**, *54*, 1705, and references cited therein.
15. Mazzucato, U.; Momicchioli, F. *Chem. Rev.* **1991**, *91*, 1679.
16. Marconi, G.; Bartocci, G.; Mazzucato, U.; Spalletti, A.; Abbate, F.; Angeloni, L.; Castellucci, E. *Chem. Phys.* **1995**, *196*, 383.
17. Shim, S. C.; Kim, M. S.; Lee, K. T.; Lee, B. H. *J. Photochem. Photobiol. A: Chem.* **1992**, *65*, 121.
18. Jeong, B. M.; Shim, S. C. *J. Photochem. Photobiol. A: Chem.* **1994**, *79*, 39.
19. Grummt, U. W.; Birkner, E.; Lindauer, H.; Beck, B.; Rotomskis, R. *J. Photochem. Photobiol. A: Chem.* **1997**, *104*, 69.
20. Shin, E. J.; Bae, E. Y.; Kim, S. H.; Kang, H. K.; Shim, S. C. *J. Photochem. Photobiol. A: Chem.* **1997**, *107*, 137.
21. Shin, E. J.; Choi, S. W. *J. Photochem. Photobiol. A: Chem.* **1998**, *114*, 23.